Articles

Synthesis and Structural Characterization of Quaternary Thorium Selenophosphates: $A_2ThP_3Se_9$ (A = K, Rb) and $Cs_4Th_2P_5Se_{17}$

Paula M. Briggs Piccoli,[†,‡] Kent D. Abney,[§] Jon R. Schoonover,[||] and Peter K. Dorhout*,[†,‡]

Department of Chemistry, Colorado State University, Fort Collins, Colorado 80523, and Nuclear Materials Technology Division, Chemical Science and Technology Division, and Materials Science and Technology Division, Los Alamos National Laboratory, Los Alamos, New Mexico 87545

Received June 30, 1999

Single crystals of $A_2ThP_3Se_9$ (A = K (**I**), Rb (**II**)) and $Cs_4Th_2PsSe_{17}$ (**III**) form from the reaction of Th and P in a molten A_2Se_3/Se (A = K, Rb, Cs) flux at 750 °C for 100 h. Compound **I** crystallizes in the triclinic space group $P\bar{1}$ (No. 2) with unit cell parameters $a = 10.4582(5)$ Å, $b = 16.5384(8)$ Å, $c = 10.2245(5)$ Å, $\alpha = 107.637(1)$; $\beta = 91.652(1)$; $\gamma = 90.343(1)°$, and $Z = 2$. Compound **II** crystallizes in the triclinic space group $P\bar{1}$ (No. 2) with the unit cell parameters $a = 10.5369(5)$ Å, $b = 16.6914(8)$ Å, $c = 10.2864(5)$ Å, $\alpha = 107.614(1)°$, $\beta = 92.059(1)°$, $\gamma = 90.409(1)°$, and $Z = 2$. These structures consist of infinite chains of corner-sharing $[Th_2Se_{14}]$ units linked by $(P_2Se_6)^{4-}$ anions in two directions to form a ribbonlike structure along the [100] direction. Compounds **I** and **II** are isostructural with the previously reported $K_2UP_3Se_9$. Compound **III** crystallizes in the monoclinic space group $P2_1/c$ (No. 14) with unit cell parameters $a = 10.238(1)$ Å, $b = 32.182(2)$ Å, $c = 10.749(1)$ Å; $\beta = 95.832(1)°$, and $Z = 4$. $Cs_4Th_2P_5Se_{17}$ consists of infinite chains of corner-sharing, polyhedral $[Th_2Se_{13}]$ units that are also linked by $(P_2Se_6)^{4-}$ anions in the [100] and [010] directions to form a layered structure. The structure of **III** features an $(Se_2)^{2-}$ anion that is bound η^2 to Th(2) and η^1 to Th(1). This anion influences the coordination sphere of the 9-coordinate Th(2) atom such that it is best described as bicapped trigonal prismatic where the η^2-bound anion occupies one coordination site. The composition of **III** may be formulated as $Cs_4Th_2(P_2Se_6)_{5/2}(Se_2)$ due to the presence of the $(Se_2)^{2-}$ unit. Raman spectra for these compounds and their interpretation are reported.

Introduction

Recent advances in solid-state chemistry of the actinide chalcogenides have seen a significant expansion of the field beyond the simple binary compounds that were studied in detail beginning in the 1940's.[1−3] In the last several years, new ternary and quaternary chalcogenide phases containing thorium and uranium have been synthesized and structurally characterized. These new complexes have resulted from the successful employment of lower temperatures and a reactive polychalcogenide flux.[4−9] This approach has given rise to a number of low-dimensional complex layered structures that have not previously been observed in actinide materials. While quaternary thorium chalcogenide compounds exist that incorporate transition metals, uranium, or lanthanides in their structures,[6,10,11] no quaternary systems of thorium had been investigated using main group cationic elements until recently, with the synthesis of $KTh_2Sb_2Se_6$.[12] Our investigation of quaternary systems containing thorium and an alkali-metal−selenium−phosphorus flux has yielded two new thorium selenophosphates: $A_2ThP_3Se_9$ (A = K (compound **I**), Rb (compound **II**)), which are isostructural to the recently reported $K_2UP_3Se_9$,[8] and a new phase, $Cs_4Th_2PsSe_{17}$ (**III**), which contains $(P_2Se_6)^{4-}$ and $(Se_2)^{2-}$ anions. In this paper, we describe these structures and compare them to their uranium counterparts as well as present Raman vibrational spectroscopic data.

Experimental Section

General Synthesis. Red phosphorus powder (99.9%) was obtained from Cerac. Selenium shot (99.999%) was purchased from Johnson Matthey. ^{232}Th ribbon was obtained from Los Alamos National

* Author to whom correspondence should be addressed at Colorado State University. Telephone: 970-491-0624. E-mail: pkd@LAMAR.colostate.edu. P.K.D. is an A. P. Sloan Fellow (1997−99) and a Camille Dreyfus Teacher Scholar (1997−99).

† Colorado State University.

‡ Nuclear Materials Technology Division, Los Alamos National Laboratory.

§ Chemical Science and Technology Division, Los Alamos National Laboratory.

|| Materials Science and Technology Division, Los Alamos National Laboratory.

(1) Zumbusch, M. *Z. Anorg. Allg. Chem.* **1940**, *243*, 322.
(2) Zachariasen, W. H. *Acta Crystallogr.* **1948**, *1*, 281.
(3) Zachariasen, W. H. *Acta Crystallogr.* **1948**, 1, 277.
(4) Sunshine, S. A.; Kang, D.; Ibers, J. A. *J. Am. Chem. Soc.* **1987**, *109*, 6202.
(5) Narducci, A. A.; Ibers, J. A. *Chem. Mater.* **1998**, *10*, 2811.
(6) Cody, J. A.; Ibers, J. A. *Inorg. Chem.* **1995**, *34*, 3165.
(7) Narducci, A. A.; Ibers, J. A. *Inorg. Chem.* **1998**, *37*, 3798.
(8) Chondroudis, K.; Kanatzidis, M. G. *C. R. Acad. Sci. Paris* **1996**, *t. 322, Ser. IIb*, 887.
(9) Chondroudis, K.; Kanatzidis, M. G. *J. Am. Chem. Soc.* **1997**, *119*, 2574.
(10) Noël, H.; Prigent, J. *Physica B + C* **1980**, *102*, 372.
(11) Sutorik, A. C.; Albritton-Thomas, J.; T., H.; Kannewurf, C. R.; Kanatzidis, M. G. *Chem. Mater.* **1996**, *8*, 751.
(12) Choi, K. S.; Iordanis, L.; Chondroudis, K.; Kanatzidis, M. *G. Inorg. Chem.* **1997**, *36*, 3804.

10.1021/ic990767w CCC: $19.00
Published on Web 06/14/2000

Laboratory, where this chemistry was realized, and the surface oxide was removed with a file before use. A_2Se_3 (A = K, Rb, Cs) were prepared from a stoichiometric ratio of the elements in liquid ammonia as described elsewhere.[13] *N,N*-Dimethylacetamide (DMA) and *N,N*-dimethylformamide (DMF) were obtained from Aldrich and used without further purification. Ampules for the reactions were all fused-silica tubes with 4 mm inner diameter and 6 mm outer diameter. All reagents were stored and manipulated in a helium-filled glovebox. Elemental analysis on single crystals that confirmed the stoichiometries was obtained from energy dispersive spectroscopy on a JEOL 6300 SEM. *Warning: ^{232}Th is a radioactive element with a half-life of 1.41 × 10^{10} years. Although its own activity is low, the inevitable daughter products of decay can render samples highly radioactive over time (γ).*

Preparation of $K_2ThP_3Se_9$ (I). K_2Se_3 (0.0386 g, 0.123 mmol), P (0.0120 g, 0.387 mmol), Se (0.0387 g, 0.490 mmol), and ^{232}Th (0.0138 g, 0.0594 mmol), in the approximate ratio of 2:6:8:1, were loaded into an ampule. The ampule was flame sealed under vacuum (<10 mTorr) and placed in a programmable furnace. The reaction was heated to 750 °C at 50 °C/h. After 100 h, the sample was cooled to 200 °C at a rate of 5 °C/h. The ampule was opened to reveal a black amorphous powder and orange crystalline reaction products that were washed with DMA to reveal the orange crystals. The products appeared to be air- and moisture-stable over several months. A single orange crystal was manually extracted from the mixture for analysis by X-ray diffraction (vide infra). This phase was also seen as a product from reaction compositions of K_2Se_3 (0.0246 g, 0.0781 mmol), P (0.0048 g, 0.155 mmol), Se (0.0431 g, 0.546 mmol), and ^{232}Th (0.0180 g, 0.0776 mmol), with the approximate ratio of 1:2:7:1, respectively, and K_2Se_4 (0.0238 g, 0.0604 mmol), P (0.0112 g, 0.3616), Se (0.0667 g, 0.8447 mmol), and ^{232}Th (0.0140 g, 0.0603 mmol) with the approximate ratio of 1:6:14:1. Yields appeared quantitative in thorium.

Preparation of $Rb_2ThP_3Se_9$ (II). Rb_2Se_3 (0.0487 g, 0.119 mmol), P (0.0073 g, 0.236 mmol), Se (0.0473 g, 0.599 mmol), and ^{232}Th (0.0277 g, 0.119 mmol), with the approximate ratio of 1:2:5:1, were loaded into an ampule and sealed under vacuum (<10 mTorr). The ampule was placed into a programmable furnace and heated to 700 °C at a rate of 50 °C/h. After 125 h, the reaction was cooled at a rate of 3 °C/h to 200 °C. The ampule was opened, and its contents were washed with DMF to reveal orange plate crystals. The products appear to be air- and moisture-stable over several months. A single orange crystal was manually extracted from the mixture for analysis by X-ray diffraction (vide infra). This phase was also seen as a product from the reaction composition Rb_2Se_3 (0.0219 g, 0.0537 mmol), P (0.0133 g, 0.429 mmol), Se (0.0633 g, 0.802 mmol), and ^{232}Th (0.0124 g, 0.0534 mmol), with the approximate ratio of 1:8:15:1, respectively. Yields appeared quantitative in thorium.

Preparation of $Cs_4Th_2P_5Se_{17}$ (III). Cs_2Se_3 (0.0435 g, 0.0865 mmol), P (0.0055 g, 0.178 mmol), Se (0.0315 g, 0.440 mmol), and ^{232}Th (0.0202 g, 0.0871 mmol), with the approximate ratio of 1:2:5:1, were loaded into an ampule. The ampule was flame sealed under vacuum (<10 mTorr) and placed in a programmable furnace. The reaction was heated to 750 °C at 50 °C/h. After 100 h, the sample was cooled to 200 °C at a rate of 4 °C/h. The ampule was opened to reveal a dark red amorphous powder and orange crystals. The solids were washed with DMF to reveal the orange crystalline product. The product appeared to be air- and moisture-stable over several months. A single orange crystal was manually extracted from the mixture for analysis by X-ray diffraction (vide infra). This phase was also seen as a product from the reaction composition Cs_2Se_3 (0.0323 g, 0.0643 mmol), P (0.0099 g, 0.320 mmol), Se (0.0456 g, 0.578 mmol), and ^{232}Th (0.0149 g, 0.0642 mmol), with the approximate ratio of 1:5:9:1, respectively. Yields appeared quantitative in thorium.

Physical Characterization. Data from single-crystal X-ray diffraction were collected on a Siemens P4 four-circle diffractometer using graphite-monochromated Mo Kα radiation and equipped with a SMART[14] system detector. Single-crystal Raman spectra were recorded using a Raman microscope system at Los Alamos National Laboratory.[15] Laser power was approximately 5 mW at the sample. The crystals from the X-ray structure determination were used in these studies.

Table 1. Crystallographic Parameters for Compounds **I**−**III**

	$K_2ThP_3Se_9$ (**I**)	$Rb_2ThP_3Se_9$ (**II**)	$Cs_4Th_2P_5Se_{17}$ (**III**)
fw	1113.79	1206.53	2492.89
temp (K)	223(2)	223(2)	223(2)
cryst system	triclinic	triclinic	monoclinic
space group	$P\bar{1}$ (No. 2)	$P\bar{1}$ (No. 2)	$P2_1/c$ (No. 14)
a (Å)	10.4582(5)	10.5369(5)	10.2378(5)
b (Å)	16.5384(8)	16.6914(8)	32.182(2)
c (Å)	10.2245(5)	10.2864(5)	10.7492(6)
α (deg)	107.637(1)	107.614(1)	90
β (deg)	91.652(1)	92.059(1)	95.832(1)
γ (deg)	90.343(1)	90.409(1)	90
V (Å^3)	1684.4(1)	1722.9(1)	3523.3(3)
Z	2	2	4
λ (Å)	0.710 73	0.710 73	0.710 73
ρ_{calc} (g/cm^3)	4.392	4.651	4.700
cryst size (mm)	0.12 × 0.12 × 0.10	0.04 × 0.06 × 0.14	0.08 × 0.08 × 0.29
μ (mm^{-1})	58.09	67.06	30.29
final R1^a/wR2^b	0.0589/0.1463	0.0476/0.1146	0.0262/0.0585
goodness of fit on F^2	1.021	1.024	1.163
secondary ext. coeff	0.0	1.2(1) × 10^{-3}	4.1(1) × 10^{-4}

^{a} $R1 = \sum|(F_o - F_c|/\sum F_o$. ^{b} $wR2 = [\sum w(F_o^2 - F_c^2)/\sum wF_c^4]^{1/2}$.

Structure Determination. Crystals were selected from the reaction mixtures and mounted in grease and placed directly into the nitrogen cold stream of the diffractometer on a glass fiber with the long axis of the crystal oriented roughly parallel to the length of the fiber. Cell constants were initially calculated from reflections taken from approximately 30 frames of reflections. Final cell constants were calculated from all reflections observed in the actual data collection. Pertinent data collection information for compounds **I**−**III** is summarized in Table 1. The data from all the data collections were processed using SAINT[16] and corrected for absorption using SADABS.[17] The structures were solved by direct methods using SHELXS-86[18] and refined in full-matrix least-squares using the program SHELXL-93.[19] All the crystals from these flux reactions suffered from small sizes and were poorly faceted, qualities that prevented us from employing analytical absorption corrections; generally, SADABS provided reasonable absorption treatments. However, for $K_2ThP_3Se_9$ (**I**), the structure initially refined to a value of $R = 0.070$, with anisotropic thermal parameters that were unusually small, and systematic discrepancies existed in the F_o to F_c lists that could not be eliminated by applying a secondary extinction coefficient. Therefore, due to the isostructural nature of **I** to the previously reported $K_2UP_3Se_9$,[8] we chose to apply the correction DIFABS[20] to reduce the residuals. Tables 2−4 give final positional parameters and equivalent isotropic displacement parameters. Tables 5 and 6 give selected bond distances and angles for **I** and **III**.

Results and Discussion

$K_2ThP_3Se_9$ (I) and $Rb_2ThP_3Se_9$ (II). The structures of **I** and **II** are isostructural with that of their previously reported U analogue, $K_2UP_3Se_9$.[8] As the structures of both **I** and **II** are identical, the main discussion will focus on $K_2ThP_3Se_9$ (**I**). The

(13) Liao, J.-H.; Kanatzidis, M. G. *Inorg. Chem.* **1992**, *31*, 431.
(14) *SMART*, 5th ed.; Siemens Analytical X-ray Systems, Inc.: Madison, WI, 1998.
(15) Schoonover, J. R.; Weesner, F.; Havrilla, G. J.; Sparrow, M.; Treado, P. *Appl. Spectrosc.* **1998**, *52*, 1505.
(16) *SAINT*, 4th ed.; Siemens Analytical X-ray Systems, Inc.: Madison, WI, 1996.
(17) Sheldrick, G. M. *SADABS*; University of Göttingen: Göttingen, Germany, 1997.
(18) Sheldrick, G. M. *Crystallographic Computing 3*; Sheldrick, G. M., Kruger, C., Doddard, R., Eds.; Oxford University Press: Oxford, U.K. 1985; pp 175.
(19) Sheldrick, G. M. *SHELXTL*, 5th ed.; Siemens Analytical X-ray Instruments, Inc.: Madison, WI, 1994.
(20) Walker, N.; Stuart, D. *Acta Crystallogr.* **1983**, *A39*, 158.

Table 2. Positional and Equivalent Isotropic Displacement Parameters for $K_2ThP_3Se_9$ (**I**)

atom	*x*	*y*	*z*	*U*(eq)[a]
Th(1)	0.2799(1)	0.1697(1)	0.7264(1)	0.009(1)
Th(2)	0.2220(1)	0.2226(1)	0.3073(1)	0.010(1)
Se(1)	0.5140(1)	0.0658(1)	0.7741(2)	0.014(1)
Se(2)	0.0555(1)	0.1494(1)	0.4964(2)	0.012(1)
Se(3)	0.4353(1)	0.1483(1)	0.4675(2)	0.012(1)
Se(4)	0.3772(1)	0.1720(1)	0.0325(2)	0.014(1)
Se(5)	0.1168(1)	0.0339(1)	0.7936(2)	0.015(1)
Se(6)	0.0791(1)	0.2854(1)	0.8771(2)	0.014(1)
Se(7)	0.2240(1)	0.3769(1)	0.2115(2)	0.017(1)
Se(8)	0.2694(1)	0.3274(1)	0.6117(2)	0.011(1)
Se(9)	0.2438(1)	−0.0160(1)	0.5095(2)	0.013(1)
Se(10)	0.4506(1)	0.3193(1)	0.8573(2)	0.016(1)
Se(11)	−0.0117(1)	0.1738(1)	0.1171(2)	0.014(1)
Se(12)	0.2301(1)	0.0307(1)	0.1372(2)	0.015(1)
Se(13)	−0.0092(1)	0.3341(1)	0.3901(2)	0.016(1)
Se(14)	0.7050(1)	0.2747(1)	0.0769(2)	0.020(1)
Se(15)	0.0326(2)	0.4812(1)	0.7841(2)	0.023(1)
Se(16)	−0.2382(1)	0.2796(1)	0.6117(2)	0.022(1)
Se(17)	0.5177(2)	0.4997(1)	0.2515(2)	0.024(1)
Se(18)	0.4845(1)	0.3125(1)	0.3766(2)	0.015(1)
P(1)	0.5037(3)	0.2832(2)	0.0401(4)	0.012(1)
P(2)	0.0843(3)	0.3516(2)	0.7205(4)	0.010(1)
P(3)	0.4332(3)	0.3782(2)	0.2252(4)	0.013(1)
P(4)	0.5757(3)	−0.0091(2)	0.5711(4)	0.011(1)
P(5)	0.0727(3)	0.0524(2)	0.0099(4)	0.009(1)
P(6)	−0.0445(3)	0.2757(2)	0.5515(4)	0.013(1)
K(1)	−0.1704(3)	0.1515(2)	0.7963(4)	0.021(1)
K(2)	0.7380(4)	0.4550(3)	−0.0494(5)	0.040(1)
K(3)	0.2550(4)	0.5332(3)	0.5278(5)	0.041(1)
K(4)	0.3085(4)	−0.1382(3)	0.7420(6)	0.049(1)

[a] *U*(eq) ($Å^2$) is defined as one-third of the trace of the orthogonalized $\mathbf{U}_{ij}$ tensor.

Table 3. Positional and Equivalent Isotropic Displacement Parameters for $Rb_2ThP_3Se_9$ (**II**)

atom	*x*	*y*	*z*	*U*(eq)[a]
Th(1)	0.2808(1)	0.1699(1)	0.7257(1)	0.011(1)
Th(2)	0.2239(1)	0.2210(1)	0.3044(1)	0.011(1)
Se(1)	0.5155(1)	0.0654(1)	0.7718(1)	0.015(1)
Se(2)	0.0585(1)	0.1482(1)	0.4932(1)	0.013(1)
Se(3)	0.4351(1)	0.1480(1)	0.4688(1)	0.013(1)
Se(4)	0.3799(1)	0.1724(1)	0.0297(1)	0.015(1)
Se(5)	0.1126(1)	0.0367(1)	0.7939(1)	0.015(1)
Se(6)	0.0834(1)	0.2877(1)	0.8721(1)	0.015(1)
Se(7)	0.2222(1)	0.3714(1)	0.2026(1)	0.016(1)
Se(8)	0.2706(1)	0.3258(1)	0.6095(1)	0.013(1)
Se(9)	0.2457(1)	−0.0139(1)	0.5126(1)	0.015(1)
Se(10)	0.4514(1)	0.3183(1)	0.8555(1)	0.017(1)
Se(11)	−0.0107(1)	0.1725(1)	0.1179(1)	0.014(1)
Se(12)	0.2320(1)	0.0314(1)	0.1328(1)	0.015(1)
Se(13)	−0.0023(1)	0.3315(1)	0.3844(1)	0.017(1)
Se(14)	0.7035(1)	0.2806(1)	0.0826(1)	0.021(1)
Se(15)	0.0283(1)	0.4775(1)	0.7694(2)	0.023(1)
Se(16)	−0.2347(1)	0.2776(1)	0.5972(2)	0.023(1)
Se(17)	0.5103(1)	0.4990(1)	0.2529(2)	0.022(1)
Se(18)	0.4815(1)	0.3119(1)	0.3741(1)	0.016(1)
P(1)	0.5034(3)	0.2842(2)	0.0401(3)	0.013(1)
P(2)	0.0849(3)	0.3500(2)	0.7124(3)	0.014(1)
P(3)	0.4294(3)	0.3777(2)	0.2237(3)	0.013(1)
P(4)	0.5754(3)	−0.0096(2)	0.5701(3)	0.012(1)
P(5)	0.716(3)	0.0528(2)	0.0082(3)	0.011(1)
P(6)	−0.0414(3)	0.2726(2)	0.5422(3)	0.014(1)
Rb(1)	−0.1723(1)	0.1533(1)	0.7961(1)	0.022(1)
Rb(2)	0.7417(1)	0.4592(1)	−0.0443(2)	0.036(1)
Rb(3)	0.2518(1)	0.5326(1)	0.5244(2)	0.029(1)
Rb(4)	0.3184(1)	−0.1293(1)	0.7593(2)	0.039(1)

[a] *U*(eq) ($Å^2$) is defined as one-third of the trace of the orthogonalized $\mathbf{U}_{ij}$ tensor.

main features of the structure consist of two crystallographically unique thorium atoms, each coordinated to 9 selenium atoms in a tricapped trigonal prismatic arrangement (Figure 1). The two polyhedra share a triangular face to form a $[Th_2Se_{14}]$ dimeric unit by sharing Se(2), Se(3), and Se(8). This dimer in turn shares its apical selenium atoms with dimers on either side to form quasi-infinite chains along the crystallographic *c*-direction. All of the selenium atoms are associated with the $(P_2Se_6)^{4-}$ anion, whose three different bonding modes in this structure have previously been described[8] and are also components in linking the dimers along the [001] direction, Figure 2. These quasi-infinite chains are joined to adjacent chains diagonally in the (101) plane, Figure 3, by $(P_2Se_6)^{4-}$ units to form aptly named "pleated" layers or slabs. These slabs are not interconnected in the [010] direction; thus, the material is considered layered. The potassium cations occupy the channels that run parallel to the chains and between the layers.

Selected bond distances and angles for $K_2ThP_3Se_9$ are found in Table 5. Th−Se bond distances range from 2.982(1) to 3.251(2) Å (average 3.102 Å), where the longest distances tend to be to the apical, or corner-sharing, selenium atom. The P−Se distances range from 2.128(4) to 2.263(4) Å (average 2.185 Å), and P−P distances range from 2.202(7) to 2.259(6) Å (average 2.222 Å). The $(P_2Se_6)^{4-}$ units are ethane-like and very regular in structure. K(1) is nine-coordinate while the other potassium cations are eight-coordinate; the K−Se distances range from 3.284(4) to 3.919(5) Å (average 3.565 Å). There are no Se−Se bonds; therefore, the oxidation states may be assigned as Th^{IV}, P^{IV}, K^{1}, and Se^{II-}.

Distances are comparable for the isostructural $Rb_2ThP_3Se_9$. Th−Se bond distances range from 2.985(1) to 3.249(1) Å (average 3.100 Å), where the longest distances tend to be to the apical, or corner-sharing, selenium atom. The P−Se distances

Table 4. Positional and Equivalent Isotropic Displacement Parameters for $Cs_4Th_2P_5Se_{17}$ (**III**)

atom	*x*	*y*	*z*	*U*(eq)[a]
Th(1)	0.2100(1)	0.1085(1)	0.1606(1)	0.010(1)
Th(2)	0.6483(1)	0.0989(1)	0.2090(1)	0.010(1)
Se(1)	0.9341(1)	0.1418(1)	0.1761(1)	0.014(1)
Se(2)	0.0298(1)	0.0802(1)	0.9373(1)	0.013(1)
Se(3)	0.4342(1)	0.1720(1)	0.1952(1)	0.012(1)
Se(4)	0.8435(1)	0.0700(1)	0.4264(1)	0.016(1)
Se(5)	0.1720(1)	0.1731(1)	0.9614(1)	0.016(1)
Se(6)	0.4407(1)	0.2530(1)	0.4348(1)	0.018(1)
Se(7)	0.6752(1)	0.1644(1)	0.4111(1)	0.016(1)
Se(8)	0.4262(1)	0.0789(1)	0.9962(1)	0.013(1)
Se(9)	0.1943(1)	0.1411(1)	0.4175(1)	0.016(1)
Se(10)	−0.0657(1)	0.1464(1)	0.6759(1)	0.017(1)
Se(11)	0.7676(1)	0.0237(1)	0.0776(1)	0.015(1)
Se(12)	0.5326(1)	0.0190(1)	0.2554(1)	0.020(1)
Se(13)	0.4243(1)	0.0728(1)	0.3536(1)	0.015(1)
Se(14)	0.6880(1)	0.1472(1)	0.9712(1)	0.017(1)
Se(15)	0.1074(1)	0.0266(1)	0.2267(1)	0.015(1)
Se(16)	0.4312(1)	0.1402(1)	0.7033(1)	0.021(1)
Se(17)	−0.0184(1)	0.2319(1)	0.3889(1,)	0.020(1)
P(1)	0.3815(2)	0.1875(1)	0.9948(21)	0.012(1)
P(2)	0.4818(2)	0.1372(1)	0.9004(21)	0.013(1)
P(3)	0.9756(2)	0.0286(1)	0.0528(2)	0.010(1)
P(4)	−0.0038(2)	0.1664(1)	0.3656(2)	0.012(1)
P(5)	0.8605(2)	0.1352(1)	0.4858(2)	0.012(1)
Cs(l)	0.1983(1)	0.2284(1)	0.6656(1)	0.020(1)
Cs(2)	0.6957(1)	0.0651(1)	0.7304(1)	0.025(1)
Cs(3)	0.6920(1)	0.2345(1)	0.6954(1)	0.031(1)
Cs(4)	0.1788(1)	0.0532(1)	0.6447(1)	0.032(1)

[a] *U*(eq) ($Å^2$) is defined as one-third of the trace of the orthogonalized $\mathbf{U}_{ij}$ tensor.

range from 2.123(3) to 2.261(3) Å (average 2.184 Å), and P−P distances range from 2.198(6) to 2.275(6) Å (average 2.230 Å). The $(P_2Se_6)^{4-}$ units are ethane-like and very regular in structure.

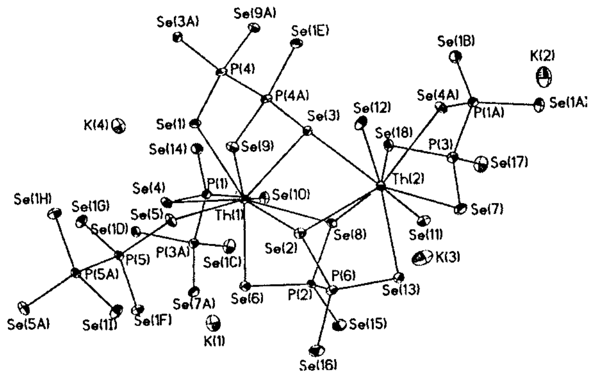

Figure 1. ORTEP rendering of the environments around Th(1) and Th(2) in $K_2ThP_3Se_9$ (50% anisotropic thermal ellipsoids). Nonbonding potassium atoms are also shown.

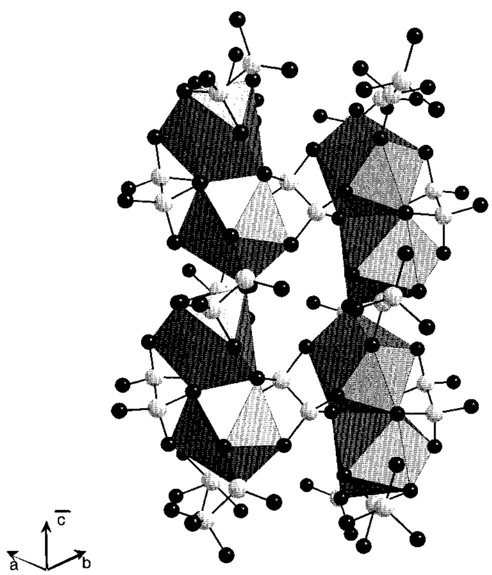

Figure 2. View down [110] of the thorium selenophosphate chains in $K_2ThP_3Se_9$ that propagate along [001]. Thorium atoms are polyhedra, filled circles are Se atoms, and gray circles are P atoms.

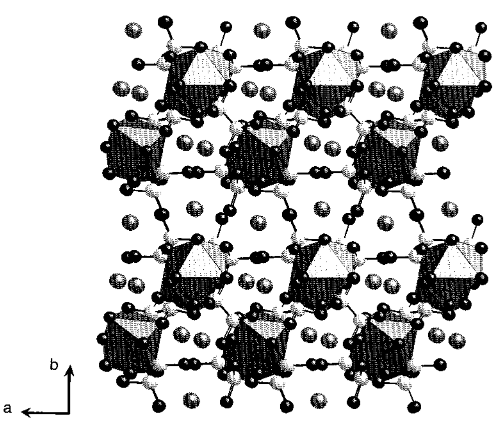

Figure 3. View down [001] of the puckered slabs in $K_2ThP_3Se_9$. Dark circles are Se atoms, light gray are P atoms, and dark gray are K atoms. Th atoms are shown as polyhedra. The slabs run left to right in the (101) plane.

Rb(1) is nine-coordinate while the other rubidium cations are eight-coordinate; the Rb−Se distances range from 3.379(2) to 4.145(2) Å (average 3.686 Å). A complete list of specific distances and angles for **II** can be found in the Supporting Information.

$Cs_4Th_2P_5Se_{17}$ (III). The structure of **III** is shown in Figure 4. Like the structure of $K_2ThP_3Se_9$ (**I**), the structure of **III** is made up of two crystallographically unique thorium atoms whose Th−Se 8- and 9-coordinate polyhedra share a triangular face to form a dimeric $[Th_2Se_{13}]$ unit. These dimers corner-share apical selenium atoms of adjacent dimers to form quasi-infinite chains that run in the [100] direction. The $(P_2Se_6)^{4-}$ units also link the dimers in the chain along [100], and they join the chains along [010] in a cross-linking fashion to form ribbons, Figure 5, in the (110) plane. There is no cross-linking in the *c*-direction to form a three-dimensional structure, and the ribbons do not link further in (110) to form the pleated sheets that were seen in compounds **I** and **II**.

Table 5. Selected Bond Distances (Å) and Angles (deg) for $K_2ThP_3Se_9$ (**I**)

Th(1)−Se(6)	2.982(1)	Th(1)−Se(10)	2.983(1)
Th(1)−Se(5)	3.062(1)	Th(1)−Se(3)	3.076(1)
Th(1)−Se(1)	3.109(1)	Th(1)−Se(8)	3.169(1)
Th(1)−Se(9)	3.210(1)	Th(1)−Se(2)	3.217(1)
Th(1)−Se(4)	3.252(2)	Th(2)−Se(7)	2.997(1)
Th(2)−Se(11)	3.026(1)	Th(2)−Se(13)	3.031(1)
Th(2)−Se(18)	3.073(1)	Th(2)−Se(8)	3.094(1)
Th(2)−Se(12)	3.127(1)	Th(2)−Se(2)	3.135(1)
Th(2)−Se(4)	3.171(1)	Th(2)−Se(3)	3.196(1)
P(2)−P(6)	2.215(6)	P(6)−Se(2)	2.263(4)
P(6)−Se(13)	2.189(4)	P(6)−Se(16)	2.130(4)
P(2)−Se(6)	2.198(4)	P(2)−Se(8)	2.238(3)
P(2)−Se(15)	2.120(4)		
Se(6)−Th(1)−Se(10)	82.70(4)	Se(6)−Th(1)−Se(5)	83.08(4)
Se(10)−Th(1)−Se(5)	142.06(5)	Se(6)−Th(1)−Se(3)	137.10(4)
Se(10)−Th(1)−Se(3)	85.83(4)	Se(5)−Th(1)−Se(3)	127.01(4)
Se(6)−Th(1)−Se(1)	141.80(4)	Se(10)−Th(1)−Se(1)	84.02(4)
Se(5)−Th(1)−Se(1)	85.82(4)	Se(3)−Th(1)−Se(1)	76.98(4)
Se(6)−Th(1)−Se(8)	72.46(4)	Se(10)−Th(1)−Se(8)	61.23(4)
Se(5)−Th(1)−Se(8)	143.95(4)	Se(3)−Th(1)−Se(8)	65.82(4)
Se(1)−Th(1)−Se(8)	129.51(4)	Se(6)−Th(1)−Se(9)	128.31(4)
Se(! 0)−Th(1)−Se(9)	148.49(4)	Se(5)−Th(1)−Se(9)	59.39(4)
Se(3)−Th(1)−Se(9)	67.70(4)	Se(1)−Th(1)−Se(9)	73.89(4)
Se(8)−Th(1)−Se(9)	117.66(4)	Se(6)−Th(1)−Se(2)	76.93(4)
Se(10)−Th(1)−Se(2)	128.82(4)	Se(5)−Th(1)−Se(2)	81.21(4)
Se(3)−Th(1)−Se(2)	78.70(4)	Se(1)−Th(1)−Se(2)	136.97(4)
Se(8)−Th(1)−Se(2)	67.93(4)	Se(9)−Th(1)−Se(2)	64.16(4)
Se(6)−Th(1)−Se(4)	83.74(4)	Se(10)−Th(1)−Se(4)	68.71(4)
Se(5)−Th(1)−Se(4)	74.89(4)	Se(3)−Th(1)−Se(4)	129.38(4)
Se(1)−Th(1)−Se(4)	58.08(4)	Se(8)−Th(1)−Se(4)	126.37(4)
Se(9)−Th(1)−Se(4)	114.88(4)	Se(2)−Th(1)−Se(4)	150.83(4)
Se(15)−P(2)−Se(6)	116.5(2)	Se(15)−P(2)−P(6)	111.3(2)
Se(6)−P(2)−P(6)	104.7(2)	Se(15)−P(2)−Se(8)	113.7(2)
Se(6)−P(2)−Se(8)	110.2(2)	P(6)−P(2)−Se(8)	98.7(2)
Se(16)−P(6)−Se(13)	114.6(2)	Se(16)−P(6)−P(2)	111.8(2)
Se(13)−P(6)−P(2)	101.7(2)	Se(16)−P(6)−Se(2)	118.2(2)
Se(13)−P(6)−Se(2)	108.0(2)	P(2)−P(6)−Se(2)	100.4(2)

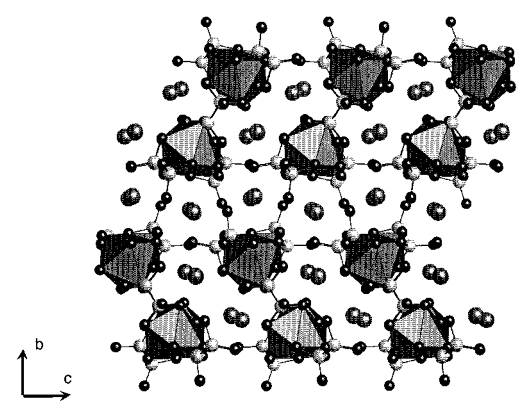

Figure 4. View of $Cs_4Th_2P_5Se_{17}$ down the $[\bar{1}00]$ direction showing the thorium polyhedra in "dumbell" ribbons that run along the $[\bar{1}00]$ direction. Dark gray circles are Cs atoms, light gray circles are P atoms, and filled circles are Se atoms.

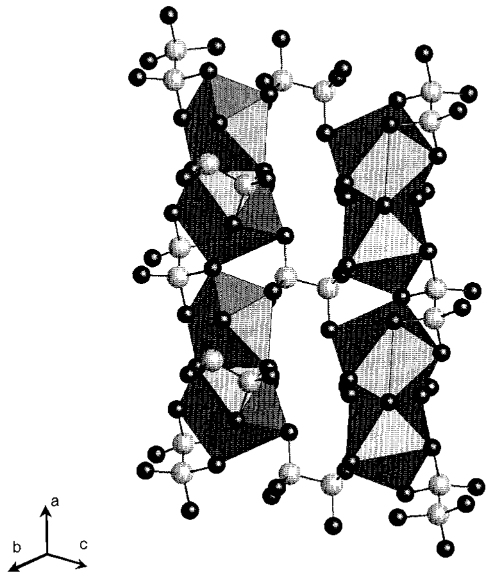

Figure 5. A view down [011] of the "dumbell" chains of thorium polyhedra linked by $(P_2Se_6)^{4-}$ units in $Cs_4Th_2P_5Se_{17}$. Filled circles are Se atoms, and gray circles are P atoms.

Th(l) is eight-coordinate with bicapped trigonal prismatic geometry. Th(2) is nine- coordinate, but does *not* appear to have the same tricapped trigonal prismatic geometry as seen in compounds **I** and **II**. Figure 6A reveals that one of the face-sharing atoms, Se(13), is within bonding distance to the terminal Se(12) at 2.362(1) Å. Neither selenium atom is within bonding distance to a phosphorus atom, and therefore, they may be formulated as an $(Se_2)^{2-}$ anion. This $(Se_2)^{2-}$ unit binds η^2 to Th(2) and η^1 to Th(1) in a bridging arrangement. While Th(2) is nine-coordinate, Figure 6B illustrates that it is best described as *bicapped trigonal prismatic* where the η^2-bound $(Se_2)^{2-}$ anion appears to occupy *one* coordination site. Dichalcogen dianions have previously been shown to occupy one coordination site in an η^2 fashion in such organometallic compounds as the tetrahedral complexes $[(\eta^5\text{-Cp})Mo(Se_2)(CO)_2]^-$,[21] $[(\eta^5\text{-Cp*})_2Re_2(Te_2)(CO)_4]$,[22] and the trigonal bipyramidal $(PPh_3)_2Os(Se_2)(CO)_2$ (Cp = C_5H_5; Cp* = C_5Me_5; Ph = C_6H_5).[23] Due to the presence of the diselenium anion, the empirical formula of the structure may be considered as $Cs_4Th_2(P_2Se_6)_{5/2}(Se_2)$.

The $(P_2Se_6)^{4-}$ anions in $Cs_4Th_2P_5Se_{17}$ have a regular ethane-like structure, and they exhibit three different bonding modes. Four bonding modes for the $(P_2Se_6)^{4-}$ anion found in actinide selenophosphates are shown in Chart 1. Modes I and II are identical to those found in $K_2UP_3Se_9$[8] and our $A_2ThP_3Se_9$ (A = K, Rb), and those modes link the corner-sharing polyhedra and cross-link the chains together, respectively. Mode III links the face-sharing polyhedra that constitute the dimer by four selenium atoms and is found in compounds **I** and **II** but not **III**. The fourth mode is only found in **III** and links the two Th atoms in the dimer. The common edge in the dimer is highlighted with a dashed line, and the dangling selenium atoms, Se(6) and Se(16), are shown.

Table 6 contains selected bond distances and angles for $Cs_4Th_2(P_2Se_6)_{5/2}(Se_2)$. Th−Se distances range from 2.8981(8) to 3.2856(8) Å (average 3.059 Å) with the longest distances

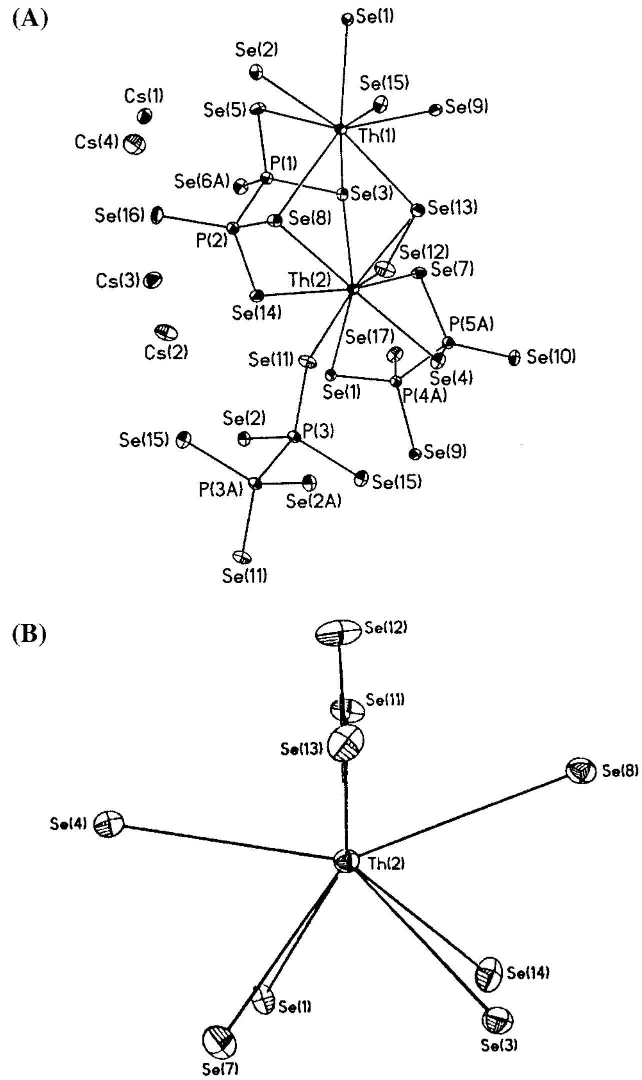

Figure 6. ORTEP plots of $Cs_4Th_2P_5Se_{17}$ (50% anisotropic thermal ellipsoids): (A) environments around Th(1) and Th(2); (B) bicapped trigonal prism around Th(2). Nonbonding Cs atoms are shown.

Chart 1

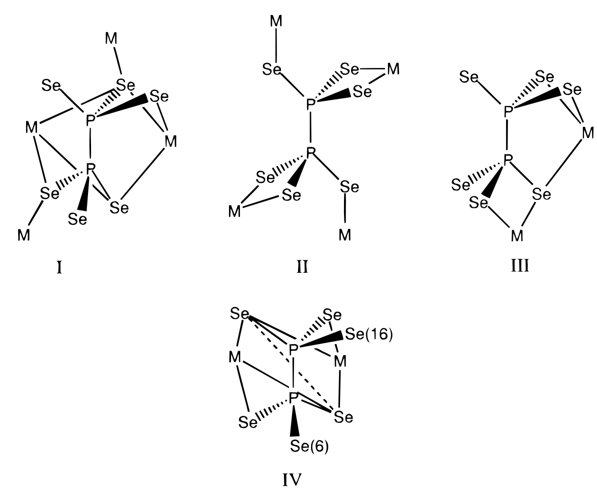

being to face- or corner-sharing selenium atoms. P−Se distances range from 2.128(2) to 2.241(2) Å (average 2.192), and P−P distances range from 2.216(3) to 2.247(3) Å (average 2.231 Å). The cesium cations, which occupy the channels that run parallel to the infinite chains and between the layers of ribbons, have

(21) Adel, J.; Weller, F.; Dehnicke, K. *J. Organomet. Chem.* **1988**, *347*, 343.
(22) Herrmann, W. A.; Hecht, C.; Herdtweck, E.; Kneuper, H.-J. *Angew. Chem., Int. Ed. Engl.* **1987**, *26*, 13.
(23) Farrar, D. H.; Grundy, K. R.; Payne, N. C.; Roper, W. R.; Walker, A. *J. Am. Chem. Soc.* **1979**, *101*, 6577.

Table 6. Se1ected Bond Distances (Å) and Angles (deg) for $Cs_4Th_2P_5Se_{17}$ (**III**)

Th(1)−Se(15)	2.9507(7)	Th(1)−Se(9)	2.9733(8)
Th(1)−Se(5)	2.9818(8)	Th(1)−Se(2)	3.0154(8)
Th(1−)Se(1)	3.0417(8)	Th(1)−Se(3)	3.0666(8)
Th(1)−Se(13)	3.0843(8)	Th(1)−Se(8)	3.1182(7)
Th(2)−Se(12)	2.8983(8)	Th(2)−Se(7)	3.0177(8)
Th(2)−Se(13)	3.0188(8)	Th(2)−Se(14)	3.0529(8)
Th(2−)Se(4)	3.0623(8)	Th(2)−Se(1111)	3.1131(7)
Th(2)−Se(8)	3.1238(8)	Th(2)−Se(3)	3.2066(8)
Th(2)−Se(1)	3.2856(8)	Se(12)−Se(13)	2.3625(10)
P(1)−P(2)	2.216(3)	P(1)−Se(3)	−2.223(2)
P(1)−Se(5)	2.187(2)	P(1)−Se(6)	2.129(2)
P(2)−Se(8)	2.241(2)	P(2)−Se(14)	2.193(2)
P(2)−Se(16)	2.133(2)		

Se(15)−Th(1)−Se(9)	92.13(2)	Se(15)−Th(1)−Se(5)	140.57(2)
Se(9)−Th(1)−Se(5)	113.93(2)	Se(15)−Th(1)−Se(2)	73.65(2)
Se(9)−Th(1)−Se(2)	139.42(2)	Se(5)−Th(1)−Se(2)	67.31(2)
Se(15)−Th(1)−Se(1)	86.93(2)	Se(9)−Th(1)−Se(1)	71.74(2)
Se(5)−Th(1)−Se(1)	74.91(2)	Se(2)−Th(1)−Se(1)	69.74(2)
Se(15)−Th(1)−Se(3)	147.78(2)	Se(9)−Th(1)−Se(3)	76.29(2)
Se(5)−Th(1)−Se(3)	70.35(2)	Se(2)−Th(1)−Se(3)	133.40(2)
Se(1)−Th(1)−Se(3)	116.52(2)	Se(15)−Th(1)−Se(13)	75.60(2)
Se(9)−Th(1)−Se(13)	66.96(2)	Se(5)−Th(1)−Se(13)	140.78(2)
Se(2)−Th(1)−Se(13)	139.35(2)	Se(1)−Th(1)−Se(13)	134.07(2)
Se(3)−Th(1)−Se(13)	72.19(2)	Se(15)−Th(1)−Se(8)	98.89(2)
Se(9)−Th(1)−Se(8)	137.92(2)	Se(5)−Th(1)−Se(8)	81.62(2)
Se(2)−Th(1)−Se(8)	82.47(2)	Se(1)−Th(1)−Se(8)	148.81(2)
Se(3)−Th(1)−Se(8)	72.90(2)	Se(13)−Th(1)−Se(8)	76.69(2)
Se(12)−Th(2)−Se(7)	120.29(2)	Se(12)−Th(2)−Se(13)	47.01(2)
Se(7)−Th(2)−Se(13)	80.92(2)	Se(12)−Th(2)−Se(14)	133.46(2)
Se(7)−Th(2)−Se(14)	103.73(2)	Se(13)−Th(2)−Se(14)	138.21(2)
Se(12)−Th(2)−Se(4)	81.06(2)	Se(7)−Th(2)−Se(4)	70.00(2)
Se(13)−Th(2)−Se(4)	89.60(2)	Se(14)−Th(2)−Se(4)	131.45(2)
Se(12)−Th(2)−Se(11)	64.77(2)	Se(7)−Th(2)−Se(11)	149.05(2)
Se(13)−Th(2)−Se(11)	111.73(2)	Se(14)−Th(2)−Se(11)	85.68(2)
Se(4)−Th(2)−Se(1)	81.62(2)	Se(12)−Th(2)−Se(8)	70.31(2)
Se(7)−Th(2)−Se(8)	132.62(2)	Se(13)−Th(2)−Se(8)	77.56(2)
Se(14)−Th(2)−Se(8)	68.97(2)	Se(4)−Th(2)−Se(8)	150.01(2)
Se(11)−Th(2)−Se(8)	78.32(2)	Se(12)−Th(2)−Se(3)	111.66(2)
Se(7)−Th(2)−Se(3)	62.23(2)	Se(13)−Th(2)−Se(3)	71.12(2)
Se(14)−Th(2)−Se(3)	74.73(2)	Se(4)−Th(2)−Se(3)	130.41(2)
Se(11)−Th(2)−Se(3)	147.82(2)	Se(8)−Th(2)−Se(3)	70.96(2)
Se(12)−Th(2)−Se(1)	140.85(2)	Se(7)−Th(2)−Se(1)	76.55(2)
Se(13)−Th(2)−Se(1)	154.67(2)	Se(14)−Th(2)−Se(1)	60.06(2)
Se(4)−Th(2)−Se(1)	71.98(2)	Se(11)−Th(2)−Se(1)	83.30(2)
Se(8)−Th(2)−Se(1)	126.72(2)	Se(3)−Th(2)−Se(1)	107.42(2)
Se(13)−Se(12)−Th(2)	69.18(3)	Se(12)−Se(13)−Th(2)	63.81(3)
Se(12)−Se(13)−Th(1)	107.89(3)	Th(2)−Se(13)−Th(1)	94.33(2)
Se(6)−P(1)−Se(5)	116.42(9)	Se(6)−P(1)−P(2)	111.01(10)
Se(5)−P(1)−P(2)	105.26(9)	Se(6)−P(1)−Se(3)	116.55(9)
Se(5)−P(11)−Se(3)	104.42(8)	P(2)−P(11)−Se(3)	101.59(9)
Se(16)−P(2)−Se(14)	117.80(9)	Se(16)−P(2)−P(1)	110.16(10)
Se(14)−P(2)−P(1)	102.03(9)	Se(16)−P(2)−Se(8)	116.55(9)
Se(14)−P(2)−Se(8)	104.13(8)	P(1)−P(2)−Se(8)	104.44(9)

irregular coordination spheres with coordination numbers of 9−12. Cs−Se distances range from 3.528(1) to 4.255(1) Å (average 3.836 Å). With one Se−Se bond per formula unit, oxidation states may be assigned as Th^{IV}, P^{IV}, and Cs^{1} (Se is found as both isolated Se^{II-} and formally as Se^{I-} in the Se_2^{2-} dimer) for a charge-balanced complex.

In a comparison of Figures 3 and 4, it is apparent that the structures of **I** and **II** are related to the structure of **III** by a missing $(P_2Se_6)^{4-}$ unit that would link the ribbons in **III** in the [011] direction into pleated sheets running along the (101) plane. The Th atoms in the pleated slabs in **I** and **II** are 8.0 and 8.3 Å apart, respectively, and form pockets in which the alkali-metal atom resides. In **III**, the distance between Th atoms in adjacent ribbons, along [011], is 9.5 Å. This increase in distance creates a hole for Cs atoms that is about 5.4 × 6.1 Å, versus the same hole in **I** for potassium that is 4.2 × 5.9 Å. The structures must accommodate the countercations within holes that are suitable

Table 7. Room-Temperature Raman Spectra of **I**−**III**

band assgnt in D_{3d}	$Mg_2P_2Se_6$[22]	$K_2ThP_3Se_9$ (**I**)	$Rb_2ThP_3Se_9$ (**II**)	$Cs_4Th_2P_5Se_{17}$ (**III**)
	86 vw	105 vw	l01 vw	102 vw
				104 vw
	114 vw			
$\nu_3(A_{1g})$	126 ms	120 vw	20 vw	118 w
		135 w	i33 w	126 w
				140 w
ν_9 (E_g)	149 s	155 m	157 m	155 m
ν_8 (E_g)	165 s	164 m	l66 m	169 w (sh)
		178 m	177 m	175 m
				182 m
				190 m
ν_2 (A_g)	222 vs	230 vs	227 vs	230 vs
	232 w		236 s	
Se−Se				283 s
?		298 vw	302 vw	304 vw
ν_7 (E_g)	462 vw	434 w	434 w	436 vw
		457 m	450 w	447 vw
		475 vw	470 vw	472 w
		482 vw	479 vw	482 w
ν_1 (A_g)	511 w	493 vw	494 vw	497 vw
		507 w	502 vw	509 vw
		516 w	517 vw	

for the alkali metals. Finally, the structures differ in formula unit. Doubling the formula unit of **I** or **II**, we get $A_4Th_2P_6Se_{18}$, which differs from **III** by a $(PSe)^{2+}$. The charge is compensated for by the formation of one $(Se_2)^{2-}$ in **III**, essentially, the loss of two negative charges that balance the loss of one $(PSe)^{2+}$ unit from the formula. For comparison, in selected reactions, the ratios of A/Th/P/Se were kept constant so that one can point to the stability of **I** and **II** versus **III** as a combination of the cation size effect and the slightly more oxidizing environment of the Cs_2Se_3/Se flux (ratio of 1:5) versus the A_2Se_3/Se flux (ratio of 1:5; A = K, Rb). This oxidizing environment in the flux favors the formation of $(Se_2)^{2-}$ without destroying the $(P_2Se_6)^{4-}$ building block. Changing the flux conditions to the more oxidizing Cs_2Se_3/Se flux (ratio of 1:15) yielded another new phase, $Cs_4Th_4P_4Se_{26}$, that contains two $(Se_2)^{2-}$ units per Th dimer and a $(P_2Se_9)^{6-}$ ligand.[24]

Raman Spectra. Room-temperature Raman data from single crystals of **I**−**III** were measured with band energies listed in Table 7. The spectra are shown in Figure 7. The spectra show striking similarities to other main-group selenophosphates $Tl_4P_2Se_6$[25] and $Mg_2P_2Se_6$,[26] and the anions may be tentatively assigned as having D_{3d} symmetry due to the relative number and intensities of the groups of resonances. Splittings within these groups occur due to the different bonding modes that the anion exhibits within the structures. Three A_{1g} and three E_g Raman active modes exist for the $[P_2Se_6]$ unit in D_{3d} symmetry.

Literature values from the aforementioned compounds[25,26] have allowed for a general assignment of the bands listed in Table 7. It must be noted that some of these bands may be of similar energies and overlap. Therefore, few of the bands can be absolutely assigned. For example, the very strong peak found around 230 cm^{-1} is well documented and assigned to the strong ν_2 (A_{1g}) stretching mode of $(P_2Se_6)^{4-}$. $Mg_2P_2Se_6$[26] provides the best assignments of the Raman active modes: ∼120−130 (ν_3, A_{1g}), ∼150 (ν_9, E_g), ∼160−170 (ν_8, E_g), ∼230 (ν_2, A_{1g}), ∼430−480 (ν_7, E_g), and ∼490−520 (ν_1, A_{1g}) for compounds **I**−**III**. Bands below 120 cm^{-1} have been assigned as lower energy

(24) Briggs Piccoli, P. M.; Abney, K. D.; Schoonover, J. R.; Dorhout, P. K. Manuscript in preparation.
(25) Brockner, W.; Ohse, L.; Pätzmann, U.; Eisenmann, B.; Schäfer, H. *Z. Naturforsch* **1985**, *40a*, 1248.
(26) Pätzmann, U.; Brockner, W. *Z. Naturforsch* **1987**, *42a*, 515.

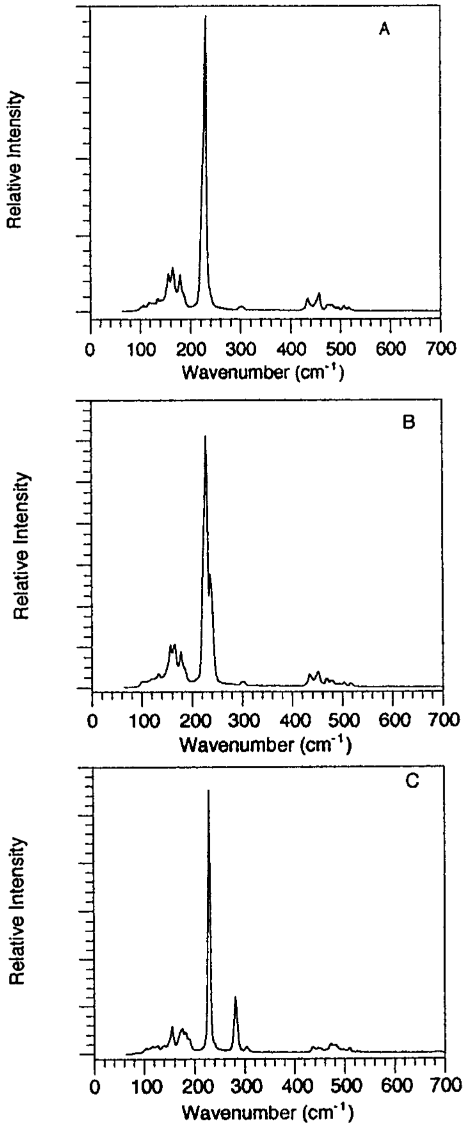

Figure 7. Single-crystal Raman spectra of (A) $K_2ThP_3Se_9$, (B) $Rb_2ThP_3Se_9$, and (C) $Cs_4Th_2P_5Se_{17}$.

phonon modes.[26] The strong band observed at 283 cm^{-1} in the spectra of $Cs_4Th_2P_5Se_{17}$ (**III**) may be assigned to the Se−Se stretch of the $(Se_2)^{2-}$ anion as this is only evident for this compound. The very weak band at ~300 cm^{-1} indicates that at least one of the $(P_2Se_6)^{4-}$ units may have C_{2h} site symmetry since this band resembles the ν_{12} (B_g) mode in $Pb_2P_2Se_6$.[27] The number of peaks (approximately 6) found for **I**−**III**, however, is lower than expected if the $(P_2Se_6)^{4-}$ units possess lower C_{2h} point group symmetry, indicating there are perhaps accidental degeneracies in the spectra. No Raman spectra have been recorded for the uranium selenophosphate phase $K_2UP_3Se_9$.[8]

(27) Becker, R.; Brockner, W. *Z. Naturforsch* **1984**, *39a*, 357.

Conclusions

The first quaternary selenophosphate phases of thorium have been prepared by the flux method and characterized by X-ray diffraction and vibrational spectroscopy. These phases support the formation of $(P_2Se_6)^{4-}$ and $(Se_2)^{2-}$ anions; we anticipate that varying the flux composition will produce new phases with other chalcophosphate or polychalcogenide anions. This approach has proven successful in other areas of solid-state synthesis involving main group elements, transition metals, and the lanthanides.[5,28−32] It is interesting to note that, on examination of the various stoichiometries of the flux compositions, the isolation of two distinctly different products from identical reaction mixtures for A = Rb and Cs were found. It appears that as the alkali-metal cation A increases in size, it allows for sufficient expansion of the structure and the oxidation chemistry of the melt supports the formation of the polychalcogenide anion $(Se_2)^{2-}$. Study in this area may lead to the rational synthesis of particular structures of interest or structures having desirable properties.

While the topics of flux composition and the role of the cation continue to be areas of focus for this project, other areas of this work include expansions of these techniques to transuranic elements such as neptunium and plutonium, where varying oxidation states will invariably lead to new structure types.

Acknowledgment. This research was supported by DOE Grant No. DE-FG03-97ER14797 and the G. T. Seaborg Institute for Transactinium Science at Los Alamos National Laboratory. P.M.B.P. gratefully thanks Dr. Brian Scott for collection of the single-crystal diffraction data, Dr. Jon Bridgewater for the collection of the Raman data, and Drs. Eduardo Garcia and David Clark for helpful discussions. The authors also acknowledge the helpful comments of the reviewers of this paper that have made this a better manuscript.

Supporting Information Available: Tables of additional crystallographic details, all bond distances and angles, and anisotropic thermal parameters. This material is available free of charge via the Internet at http://pubs.acs.org.

IC990767W

(28) Kanatzidis, M. G. *Curr. Opin. Solid State Mater. Sci.* **1997**, *2*, 139.
(29) Sutorik, A. C.; Kanatzidis, M. G. *Chem. Mater.* **1997**, *9*, 387.
(30) Chondroudis, K.; Kanatzidis, M. G. *Inorg. Chem.* **1998**, *37*, 3792.
(31) Chen, J. H.; Dorhout, P. K. *Inorg. Chem.* **1995**, 34, 5705.
(32) Chen, J. H.; Dorhout, P. K.; Ostenson, J. E. *Inorg. Chem.* **1996**, *35*, 5627.